Nuclear Materials and Energy 38 (2024) 101583

Contents lists available at ScienceDirect

Nuclear Materials and Energy

journal homepage: www.elsevier.com/locate/nme

Comparative analysis of gas release from biphasic lithium ceramics pebble beds of various pebbles sizes and content under neutron irradiation conditions

Timur Kulsartov [a,b], Zhanna Zaurbekova [a,b,*], Regina Knitter [c], Inesh Kenzhina [a,b], Yevgen Chikhray [a,b], Asset Shaimerdenov [b], Saulet Askerbekov [a,b], Gunta Kizane [d], Alexandr Yelishenkov [a], Timur Zholdybayev [b]

[a] Satbayev University, Almaty, Kazakhstan
[b] Institute of Nuclear Physics, Almaty, Kazakhstan
[c] Karlsruhe Institute of Technology, Karlsruhe, Germany
[d] University of Latvia, Riga, Latvia

ARTICLE INFO

Keywords:
Lithium ceramics
Helium
Tritium
Neutron irradiation
Breeder blanket

ABSTRACT

This paper presents the results of 4 reactor campaigns on the irradiation of biphasic lithium ceramics containing different ratios of lithium orthosilicate (LOS) and lithium metatitanate (LMT) components (25 and 35 mol% LMT in LOS). The size distribution of pebbles in pebble beds was 250–1250 μm and 500–710 μm, respectively. The studies were carried out sequentially with each type of ceramics. In experiments carried out using the vacuum extraction method, the composition of gases released from lithium ceramic samples was registered in in-situ mode. The absence of purge gas during the experiments minimized the possibility of T_2O and HTO formation, significantly simplifying processing of the results and providing more opportunities for results analysis. The main goal of the present paper was to identify the general patterns of the release of gases with mass numbers M2 (H_2), M4 (He + HT), M6 (T_2) and M18 (H_2O) from ceramic samples throughout the entire irradiation experiment in 4 campaigns. Release trends of main gases with mass numbers M2, M4, M6 and M18 for all four campaigns are presented and their comparative analysis was performed. The average partial pressure of tritium release in the form of T_2 and HT molecules for all campaigns was determined as 5.8×10^{-7} Torr. The dependences of formation rates of helium release peaks on the irradiation time were plotted. The nature of peak emissions does not have a monotonic relationship; upon irradiation, both an increase in the frequency of peaks and a decrease in it are observed. During irradiation, the process of peak helium release does not stop.

The simulation was carried out by the finite element method, assuming that tritium release from the sample is determined by diffusion and desorption processes from the sample surface. The experimental curves are satisfactorily described by a number of sets of desorption and diffusion parameters. One way or another they lie in the range of specified values. The Arrhenius dependences of the effective diffusion coefficient and desorption coefficient obtained for lithium ceramics 35 LMT are equal to:

$$D = 5,2 \times 10^{-11} \left(\frac{m^2}{s}\right) \exp\left(\frac{-21\left(\frac{kJ}{mole}\right)}{RT}\right),$$

$$K = 1.21 \times 10^{-4} \left(\frac{m^2}{s}\right) \exp\left(\frac{-64\left(\frac{kJ}{mole}\right)}{RT}\right).$$

The values of the effective diffusion coefficient and tritium desorption coefficient in 25 LMT ceramics were 15 and 20% lower than in 35 LMT ceramics.

* Corresponding author.
E-mail address: zzha@physics.kz (Z. Zaurbekova).

https://doi.org/10.1016/j.nme.2024.101583
Received 10 November 2023; Received in revised form 19 December 2023; Accepted 4 January 2024
Available online 6 January 2024
2352-1791/© 2024 The Authors. Published by Elsevier Ltd. This is an open access article under the CC BY-NC-ND license (http://creativecommons.org/licenses/by-nc-nd/4.0/).

1. Introduction

Taking into account the current level of technology development, the fusion reaction of deuterium and tritium light nuclei D + T = He (3.5 MeV) + n (14.1 MeV) is the most accessible and effective reaction for use in fusion reactors.

To implement a closed fuel cycle of a fusion reactor operating on DT-fuel, it is necessary to produce tritium inside the fusion facility itself. For these purposes lithium-containing materials are used in the breeder blanket and tritium is produced from lithium under neutron irradiation by the reaction $^{6}Li(n,\alpha)T$. In solid breeder concept the tritium formed is collected using a purge gas, and then, after extraction and purification, is fed into the fusion reactor chamber and used as a fuel.

Biphasic lithium ceramics based on lithium orthosilicate Li_4SiO_4 (LOS) and lithium metatitanate Li_2TiO_3 (LMT) are one of the most promising materials for breeder blankets of future fusion reactors [1–6]. LMT and LOS have low activation compared to lithium zirconate Li_2ZrO_3 and lithium aluminate $LiAlO_2$ and have satisfactory thermo-mechanical and chemical properties [7–10]. Tritium generation in Li_4SiO_4 is higher than in Li_2TiO_3 due to the higher density of lithium atoms, but data on tritium release for Li_4SiO_4 vary greatly [11–13]. The concept of a biphasic mixture of Li_2TiO_3 and Li_4SiO_4 was developed by the authors of [14], in order to realize the beneficial complementarity of these materials. Later, the authors of [5,6] proposed their approaches to the production of this material. The authors of [15] proposed adding lead to the composition of biphasic lithium ceramics in order to increase the efficiency of tritium generation without increasing the lithium content, since it negatively affects the chemical inertness of the ceramics.

Today very little information is available on the evaluation of tritium release from biphasic lithium ceramics. However, this criterion is one of the key parameters in the final choice of breeder material. Most experiments on tritium release from ceramics are carried out according to the following scheme: the material is irradiated in a fission reactor, and then the release of accumulated tritium is separately studied in post-irradiation examinations (PIE). Such experiments were carried out with pebbles Li_2TiO_3-Li_4SiO_4 [16] and Li_2TiO_3–0.5Li_4SiO_4 [17], with sintered powders Li_2TiO_3–0.5Li4SiO_4 [18], Li_2TiO_3–0.5Li_4SiO_4 [19] and Li_2TiO_3-0.5Li_4SiO_4–Pb [20], with Li_2TiO_3-Li_4SiO_4 pebbles coated with a layer of Li_2TiO_3 [21]. In [22], gas evolution from biphasic lithium ceramic pebbles of various compositions (20–30 mol% LMT in LOS) pre-saturated with tritium was studied.

Interpretation of PIE results is quite complex, and does not take into account how changes in irradiation conditions affect the processes of tritium release in real time (such processes as diffusion in crystal grains, capture/release in radiation traps, association/dissociation with other atoms, adsorption/desorption on surface of the material). Also, in these works, the amount of helium released from the samples was not measured (which is produced from lithium in the same amount as tritium). Helium production is an important process, which subsequently causes various irreversible changes in ceramics.

This paper presents the results of 4 reactor campaigns on the irradiation of biphasic lithium ceramics containing different ratios of LMT and LOS components (25 and 35 mol% lithium metatitanate). The size distribution of the pebbles was 250–1250 μm and 500–710 μm, respectively. The studies were carried out sequentially with each type of ceramics. In experiments carried out using the vacuum extraction method, the composition of gases released from lithium ceramic samples was registered in in-situ mode. The absence of purge gas during the experiments minimized the possibility of T_2O and HTO formation, significantly simplifying processing of the results and providing more opportunities for results analysis.

Previously, in [23,24], a comparison of the initial sections of reactor experiments was made for all campaigns, where the reactor was sequentially brought to power. However, the main goal of the present paper was to identify the general patterns of the release of gases with mass numbers M2 (H_2), M4 (He + HT), M6 (T_2) and M18 (H_2O) from ceramic samples throughout the entire irradiation experiment in 4 campaigns.

2. Materials and method

Four successive irradiation campaigns were carried out with lithium orthosilicate samples of various sizes containing 25 and 35 mol% of lithium metatitanate, respectively.

Ceramic samples were manufactured at KIT using the melt-based KALOS process [4]. In this process first lithium hydroxide monohydrate ($LiOH{\cdot}H_2O$), silicon dioxide (SiO_2) and titanium dioxide (TiO_2) were mixed and then subjected to heat treatment to remove residual water. The resulting composition was then poured into a platinum alloy melting crucible. The mixture was heated to a temperature of 1300–1400 °C (depending on the composition) and fed through a nozzle, forming drops. Then the droplets were cooled with liquid nitrogen to solidify. The main parameters of the samples are given in Table 1 and in Fig. 1, more detailed information about the method is given in [4]. The size range of the pebbles was the standard fraction of 250–1250 μm, or screened to the range of 500–710 μm, respectively. Irradiation of pebble beds of various sizes is due to the interest associated with the fact that for different pebble beds the packing factor will be different [25], and the kinetics of tritium release will be determined by a combination of parameters: the packing factor and the geometric dimensions of the pebbles themselves (and their quantitative distribution in the pebble bed).

Experiments were carried out at the CIRRA (Complex of In-Reactor gas Release Analysis) facility [24,26–29], located at the WWR-K research reactor in Institute of Nuclear Physics, Almaty, Kazakhstan. The neutron spectrum of the WWR-K reactor is shown in Fig. 2. The experimental facility can be structurally divided into four key elements: the reactor ampoule device (AD) with the samples; the vacuum path and the pump-out system (including wide-range pressure sensors EdwardsWRG-NW25 with an accuracy of 15 % for pressures below 100 mbar and 30 % for pressures below 1 μbar); the RGA-100 residual gas analyzer (with an accuracy of 10 %), as well as the gas inlet system, which uses a leaking valve to supply controlled gas flows into the chamber with samples during the experiment.

Three thermocouples of chromel–alumel type (with accuracy ± 1 °C) were installed on the walls and bottom of the AD to measure the temperature. Then this assembly was placed in the dry experimental channel of the reactor. The design makes it possible to use the AD several times. The samples were located in AD at the core center level.

A sample of the pebble bed was placed in a stainless steel capsule, which was inserted into an evacuated irradiation ampoule device (Fig. 3). The experiment was carried out using the vacuum extraction method, during which the capsule with the sample was continuously pumped out by a turbomolecular pump at a speed of 100 l/s. Under such conditions, tritium leakage, i.e. its migration through the capsule walls

Table 1
Main parameters of Li_2TiO_3-Li_4SiO_4 pebbles.

	1st campaign	2nd campaign	3rd campaign	4th campaign
Samples	25 LMT «Standard» (lithium orthosilicate with 25 mol% lithium metatitanate	35 LMT «Standard» (lithium orthosilicate with 35 mol% lithium metatitanate)	35 LMT «500 −710 μm» (lithium orthosilicate with 35 mol% lithium metatitanate)	25 LMT «500 −710 μm» (lithium orthosilicate with 25 mol% lithium metatitanate)
Pebble size, μm	250–1250	250–1250	500–710	500–710
Irradiation time, days	5	22	22	15
Weight, g	5.0266	5.0116	5.0233	5.0780

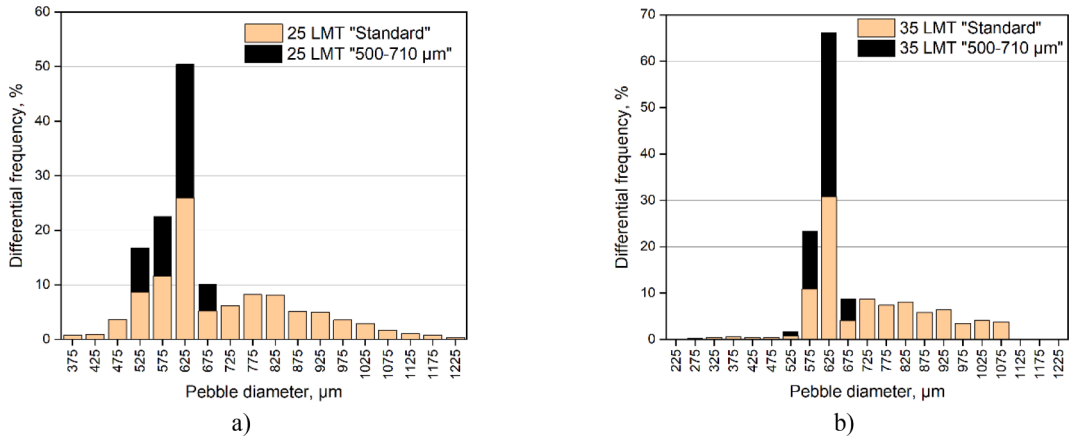

Fig. 1. Pebble size distribution of the irradiated ceramic samples: a) 25 LMT; b) 35 LMT.

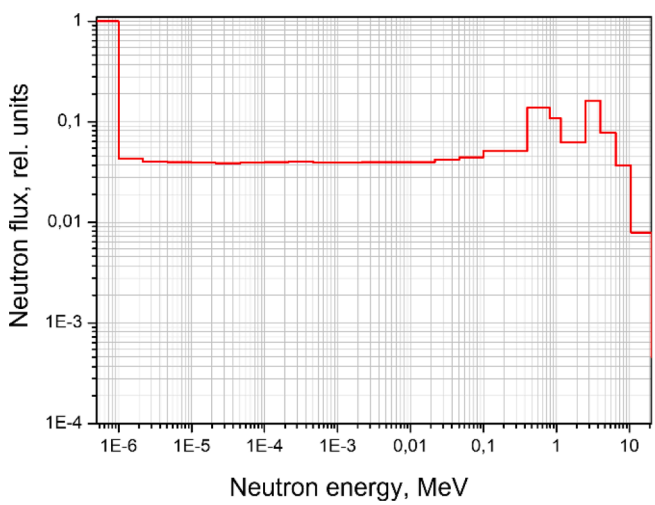

Fig. 2. Neutron spectrum of the WWR-K reactor.

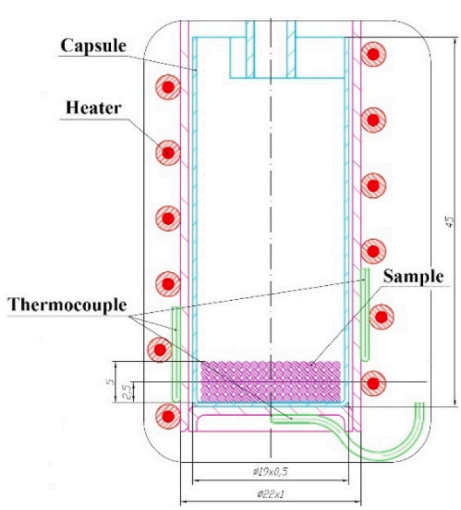

Fig. 3. Irradiation ampoule device with capsule.

was considered negligible. Irradiation was carried out according to the scheme described in detail in [24]. First, the reactor was brought to the thermal power levels of 1, 3, 4.8 and 6 MW, then further irradiation occurred at 6 MW for the time periods indicated in Table 1. The average temperature of the ceramics during irradiation was about 680 °C.

3. Results and discussion

3.1. Results of reactor experiments

Fig. 4 shows the diagrams of all four irradiation campaigns for samples of biphasic lithium ceramics at the WWR-K reactor. The diagrams, shown on the same scale for convenience of comprehension, reflect the time dependences of the release of gases with the following masses from the sample: M2, which corresponds to the release of hydrogen H_2; M4, which corresponds to the release of gases HT and He; M6, which corresponds to the release of tritium in the form of molecule T_2 and M18, which corresponds to the release of water vapor H_2O.

The authors assume that the main release of tritium from the sample occurs in the form of HT (blue line on the graph in Fig. 4) and T_2 (purple line) molecules. The release of tritium in the form of tritiated water HTO amounted to no more than 5 % of the total amount of tritium and is not reflected on the graph. According to the authors, the ratio between the amount of HT, T_2, and HTO molecules depends on the partial pressure of hydrogen in the experimental chamber and the concentration of adsorbed water molecules on the ceramic surface.

The presence of H_2O and H_2 gases is explained by their unavoidable presence in the structural materials of the ampoule device and the experimental capsule with the sample. The graphs show that the level of these gases is approximately the same in each campaign and is of the order of $5{\cdot}10^{-6}$ Torr, and then there is a decrease in this level to $5{\cdot}10^{-7}$ Torr by the end of irradiation.

During irradiation in each campaign, additional experiments were conducted with changes in irradiation parameters (temperature, reactor power), as well as with the supply of different gases such as deuterium, hydrogen, carbon dioxide, and water vapor to the experimental chamber with the sample. Such plots are depicted as gaps in the general diagrams of the experiment. The results of the analysis of these irradiation sites are given in [23,30,31]. The site where the gradual shutdown of the reactor in the second campaign took place is discussed in detail in [32].

In this paper, the focus is on examining the trends of major gas release from two-phase lithium ceramic samples simultaneously for all four campaigns and comparing them.

When interpreting the obtained results of changes in the gas composition in the chamber during irradiation, was authors of the present paper suggested that the release of the M4 peak can be decomposed into two components. One of them, responsible for the release of HT molecule (Fig. 5, in red), represents the lower level of the M4 release curve. And the second one, responsible for the variable component, refers to the peak release of helium from the ceramic. The release of tritium-containing molecules (HT and T_2) from sample during the experiment should be observed simultaneously, i.e. if the peak release of gas with mass M4 is an HT molecule, then the release of M6

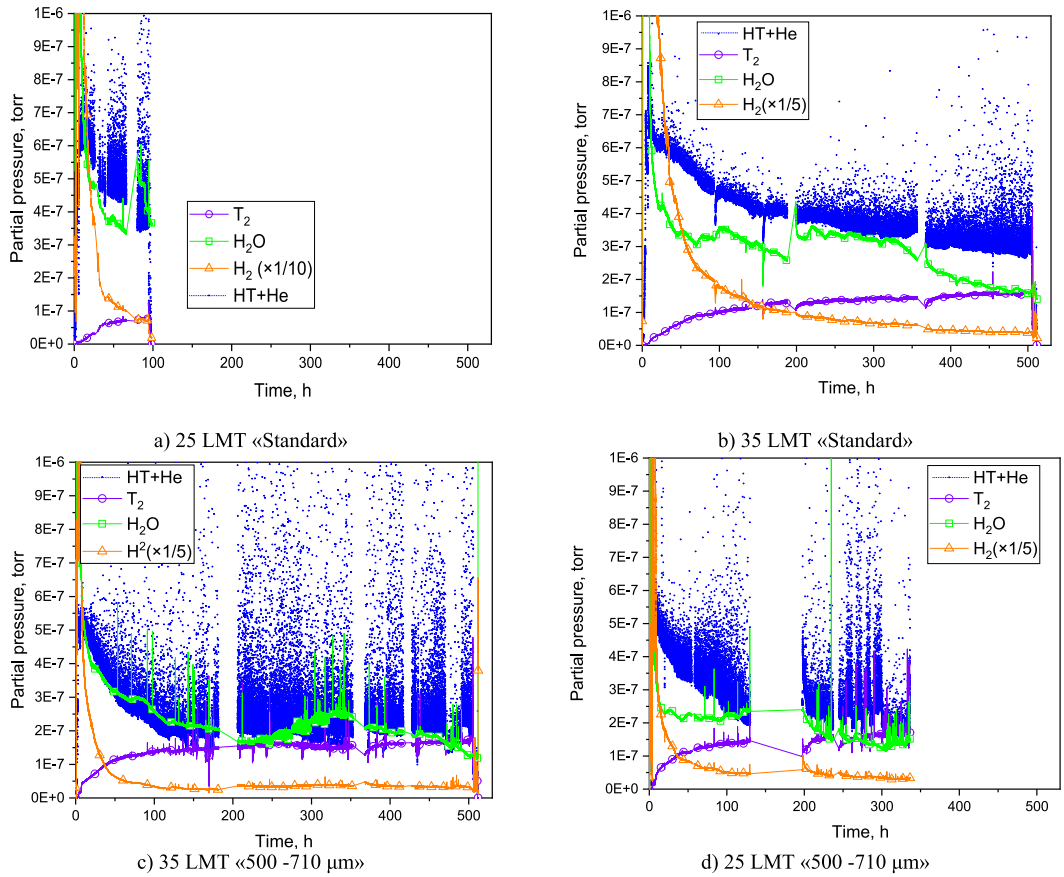

Fig. 4. Diagrams of reactor experiments with different samples of biphasic lithium ceramics.

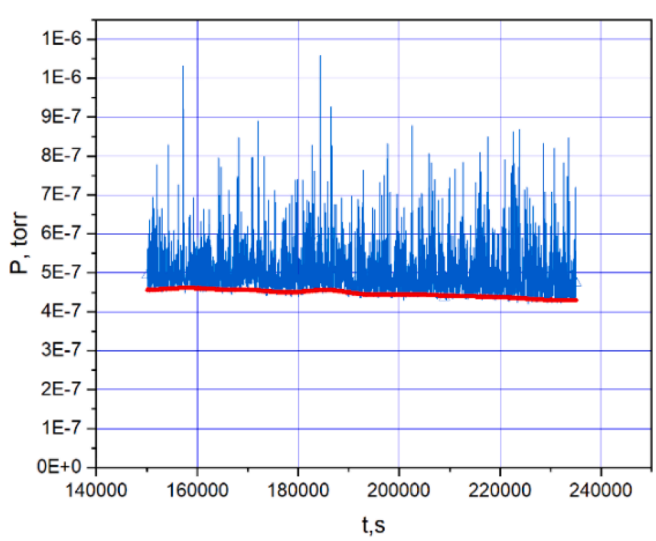

Fig. 5. Enlarged section of the M4 mass release diagram (HT level is marked in red). (For interpretation of the references to colour in this figure legend, the reader is referred to the web version of this article.)

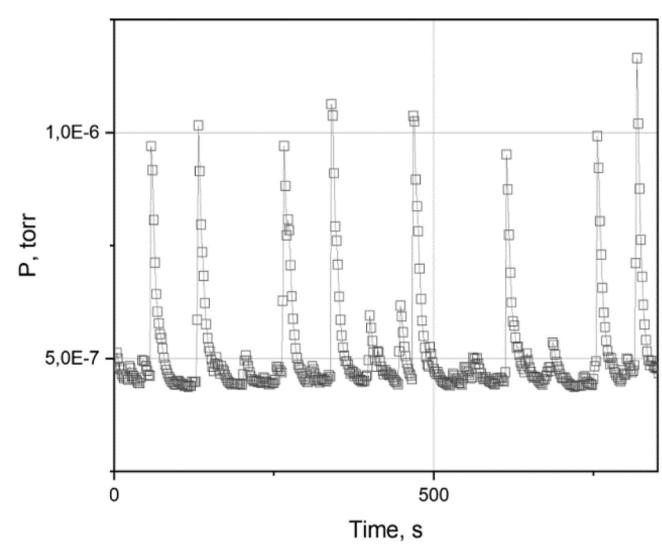

Fig. 6. Pulses of gas release peaks with mass number M4 [29].

(T_2) should also be of a peak nature. But in the experiment, it is not observed bursts in the release of the M6 mass, from which the authors made the assumption that the gas released in the form of peaks is He, which is formed in lithium in the same amount as tritium. The amplitude of the peaks increases with increasing irradiation time. The shape of helium peaks in enlarged scale is shown in Fig. 6.

The kinetics of the release of the main tritium-containing gases, as well as the peculiarities of helium release from the sample, depend on the conditions and duration of irradiation.

3.2. Analysis of gas release trends from ceramics

Next, diagrams describing the main trends in the release of gases with mass numbers M2, M4, M6, and M18 from the lithium ceramic sample were plotted (Fig. 7).

Using the example of the second campaign, it can be observed that,

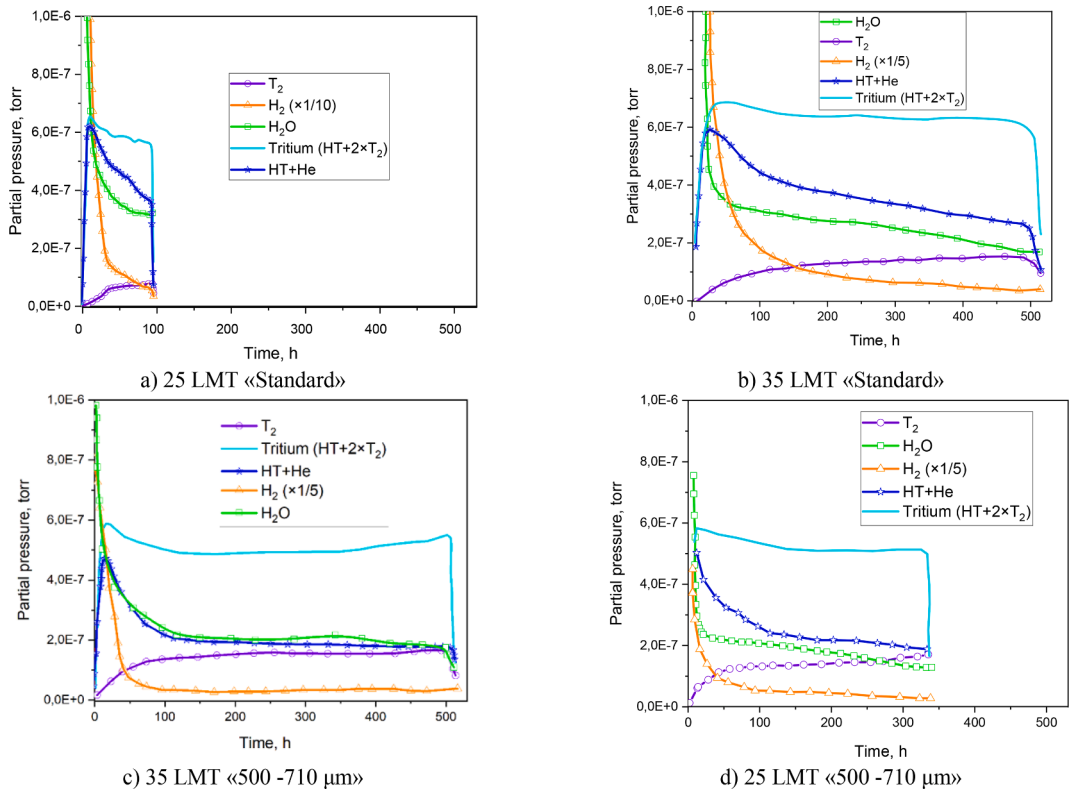

Fig. 7. Main trends in the release of gases with mass numbers M2, M4, M6 and M18 from samples of biphasic lithium ceramics during irradiation.

despite the decrease in the level of the M4 mass (blue line in Fig. 7 b), responsible for the release of HT and He, and the increase in the level of tritium in the form of the T_2 molecule (purple), the total tritium level, accounting for the release of tritium atoms in the form of HT and T_2 molecules (turquoise line in Fig. 7 b), remains approximately constant. This pattern is observed for all 4 campaigns. The value of this level of tritium partial pressure is also approximately the same for all experiments and is about $5.8 \cdot 10^{-7}$ Torr (which is expected, since the mass of ceramics loaded into the capsule was approximately the same and was about 5 g). This means that on the ceramic surface the number of tritium atoms increases to a certain level and remains constant, while the number of hydrogen atoms decreases continuously. As noted above, hydrogen atoms on the ceramic surface appear as a result of adsorption-dissociation processes of hydrogen and water vapor from the gas phase. Therefore, it can be said that during irradiation there is a gradual decrease of hydrogen and water vapor pressure in all experiments.

At the initial stages of irradiation, the proportionality between the decrease in the pressures of gases H_2, H_2O, HT + He and the increase in the pressure of gas T_2 is quite well observed. However, over time, this proportionality begins to break down somewhat. In this connection, our assumption that the release of gas with mass number M4 does not contain a uniform helium release over the entire campaign period, but only peak releases, needs additional verification.

This is due to the fact that our attempts to describe the processes at the surface showed that at the observed significant drop in the hydrogen and water vapor pressures in the chamber, the recorded HT gas pressure should have become less than the T_2 gas pressure by the end of the experiment. We see that for campaigns 3 and 4 these pressures are almost comparable, but do not reach the expected ratio. According to our estimates, at the end of the campaign, the helium content can be up to 25 % of the total pressure of the gas with mass number M4.

3.3. Helium peak release analysis

Next, the dependences of the formation rate of helium peaks on the irradiation time were plotted (Fig. 8). Here, the average tritium release level ($5.8 \cdot 10^{-7}$ Torr) was chosen as a characteristic of the level that determines the magnitude of the peaks (since the amount of tritium and helium produced in ceramics is the same). Further calculations took into account helium peak releases exceeding this level by at least 20 %.

Data are presented for peaks ranging from 20 to 40 %, from 40 to 60 %, from 60 to 80 %, from 80 to 100 % and above 100 % of the selected level. Peak counting was carried out for the entire duration of the each campaign.

In general, the data presented in Fig. 8 formalize the following features of the peak helium release during the experiment:

- In general, peak emissions in the range of 20–40 % predominate throughout the entire campaign period for all samples and do not exceed a frequency of 12 peaks per hour.
- Peaks of helium release in the range of 80–100 % and above 100 % appear after a significant irradiation time (more than 50–100 h).
- The nature of peak emissions does not have a monotonic relationship; upon irradiation, both an increase in the peak's frequency and a decrease in it are observed.
- When irradiated, the process of peak release of helium does not stop, as, for example, it occurs with lithium metatitanate in similar experiments conducted earlier [33] (shown in Fig. 9). From our point of view, this is due to the process of helium escaping from open pores on the surface of the pebble. The process of increasing open porosity is predominant, since the rate of helium and tritium release from the ceramics increases as irradiation proceeds. It is impossible without additional research to assess the extent to which this process affects the structure of pebbles, but it has a positive effect on the yield of tritium from ceramics.

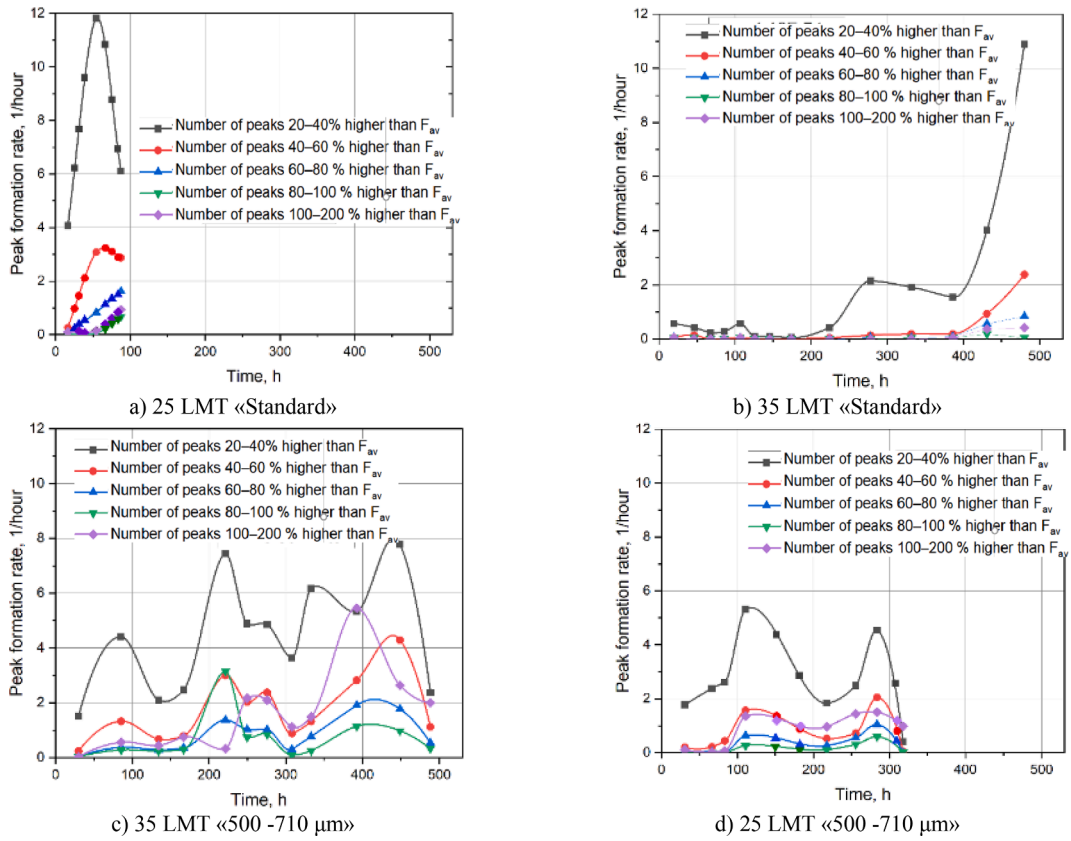

Fig. 8. Helium peaks formation rate biphasic lithium ceramics samples during irradiation campaigns.

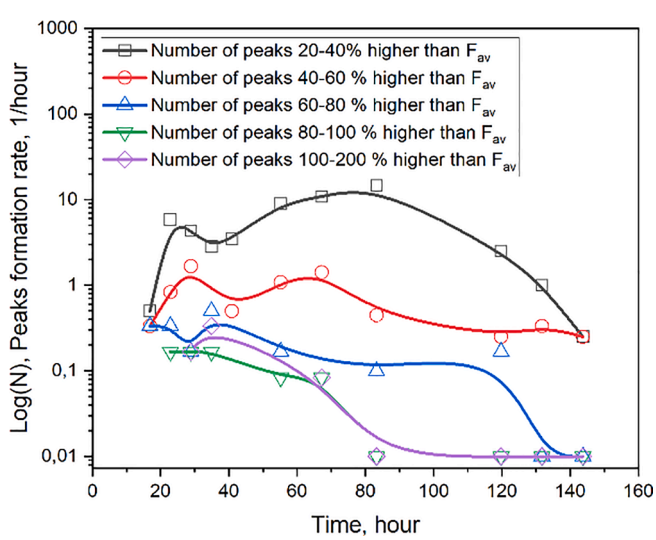

Fig. 9. Time dependence of the rate of helium peak release from lithium metatitanate [33].

3.4. Results of simulation of tritium release from ceramics

The next stage of the work was simulation of the process of tritium release from biphasic ceramic samples at the initial stage of irradiation, including the first 8.5 h. During this period, the reactor was stepwise brought to the power of 1, 3, 4.8 and 6 MW. At the same time, the temperature of the samples was changed due to radiation heating.

The simulation was carried out by the finite element method using the COMSOL Multiphysics software package [34], assuming that tritium release from the sample is determined by diffusion and desorption processes from the sample surface. Four parameters were varied in the model: the parameters of the Arrhenius dependence of the tritium diffusion coefficient D_0 and E_{dif}, and the desorption rate constants of tritium molecules K_0, E_{des} corresponding to expressions (1) and (2):

$$D = D_0 exp\left(-\frac{E_{dif}}{RT}\right), \tag{1}$$

$$K = K_0 exp\left(-\frac{E_{des}}{RT}\right), \tag{2}$$

where D_0 (m^2/s) is the pre-exponent in the Arrhenius dependence of the tritium diffusion coefficient; E_{dif} is the diffusion activation energy (kJ/mol); K_0 (m^2/(mole·s)) is the pre-exponent in the Arrhenius dependence of the tritium desorption rate constant; E_{des} is the activation energy of desorption of tritium molecules HT and T_2 (kJ/mol).

Varying 4 parameters for the model simultaneously would result in a large number of these parameters sets that would satisfactorily describe the experimental curve.

To obtain a unique (single) set of these parameters it was decided to divide the simulation procedure into 2 stages, with determination/estimation of at least 2 parameters in the first stage and 2 parameters in the second stage of simulation.

At the first stage of simulation, the estimated parameters of diffusion coefficients were obtained assuming that tritium release is determined only by diffusion processes in ceramic samples (i.e., diffusion is the limiting process). The changes of tritium concentration in the samples as well as the tritium flux from them were determined. The obtained values of the diffusion coefficient parameters were used as estimates for the diffusion-desorption model, which was further used to describe tritium release at the second stage of simulation. A detailed description of the simulation process of tritium release from ceramics determined by the diffusion-desorption approximation is given in [32].

Fig. 10 shows the results of tritium release simulation as a T_2 molecule. The experimental curves are satisfactorily described by a number of sets of desorption and diffusion parameters, they are within the range of the given values.

The Arrhenius dependences of the effective diffusion coefficient and desorption coefficient obtained for 35 LMT lithium ceramics are found to be equal to:

$$D = 5,2 \times 10^{-11}\left(\frac{m^2}{s}\right)\exp\left(\frac{-21\left(\frac{kJ}{mole}\right)}{RT}\right),$$

$$K = 1.21 \times 10^{-4}\left(\frac{m^2}{s}\right)\exp\left(\frac{-64\left(\frac{kJ}{mole}\right)}{RT}\right).$$

The values of effective diffusion coefficient and tritium desorption coefficient of 25 LMT ceramics were 15 and 20 % lower than those of 35 LMT ceramics.

Authors suggested that one of the possible mechanisms of tritium release from ceramics is a mechanism related to both diffusion and desorption of tritium from the pebble surface and tritium release from the open pores of the pebbles.

4. Conclusions

Reactor experiments were carried out with 4 different samples of biphasic lithium ceramics. During irradiation, gases released from the samples was registered by the mass spectrometric registration system.

Release trends of main gases with mass numbers M2, M4, M6 and M18 for all four campaigns are presented and their comparative analysis was performed.

The average partial pressure of tritium release in the form of T_2 and HT molecules for all campaigns was determined as 5.8×10^{-7} Torr.

The dependences of formation rates of helium release peaks on the irradiation time were plotted. The nature of peak emissions does not have a monotonic relationship; upon irradiation, both an increase in the frequency of peaks and a decrease in it are observed. During irradiation, the process of peak helium release does not stop.

The experimental curves are satisfactorily described by a number of sets of desorption and diffusion parameters. Simulation within the framework of the desorption and diffusion model made it possible to describe the obtained dependences of tritium release in the region of the beginning of irradiation for each reactor experiment and determine the Arrhenius dependences of the effective diffusion coefficient and desorption coefficient for lithium ceramics 35 LMT and 25 LMT. The values of the effective diffusion coefficient and tritium desorption coefficient in 25 LMT ceramics were 15 and 20 % lower than in 35 LMT ceramics.

It is planned, based on new experimental data and using an approach that takes into account the porosity of the pebbles, to confirm (or refute) the mechanism proposed in the presented work for the release of tritium from ceramics, associated with both diffusion and desorption of tritium from the surface of the pebbles, as well as the release of tritium from the open pores of pebbles.

Thus, as reactor experiments have shown, the release of tritium from the studied biphasic lithium ceramics of different types occurs in a

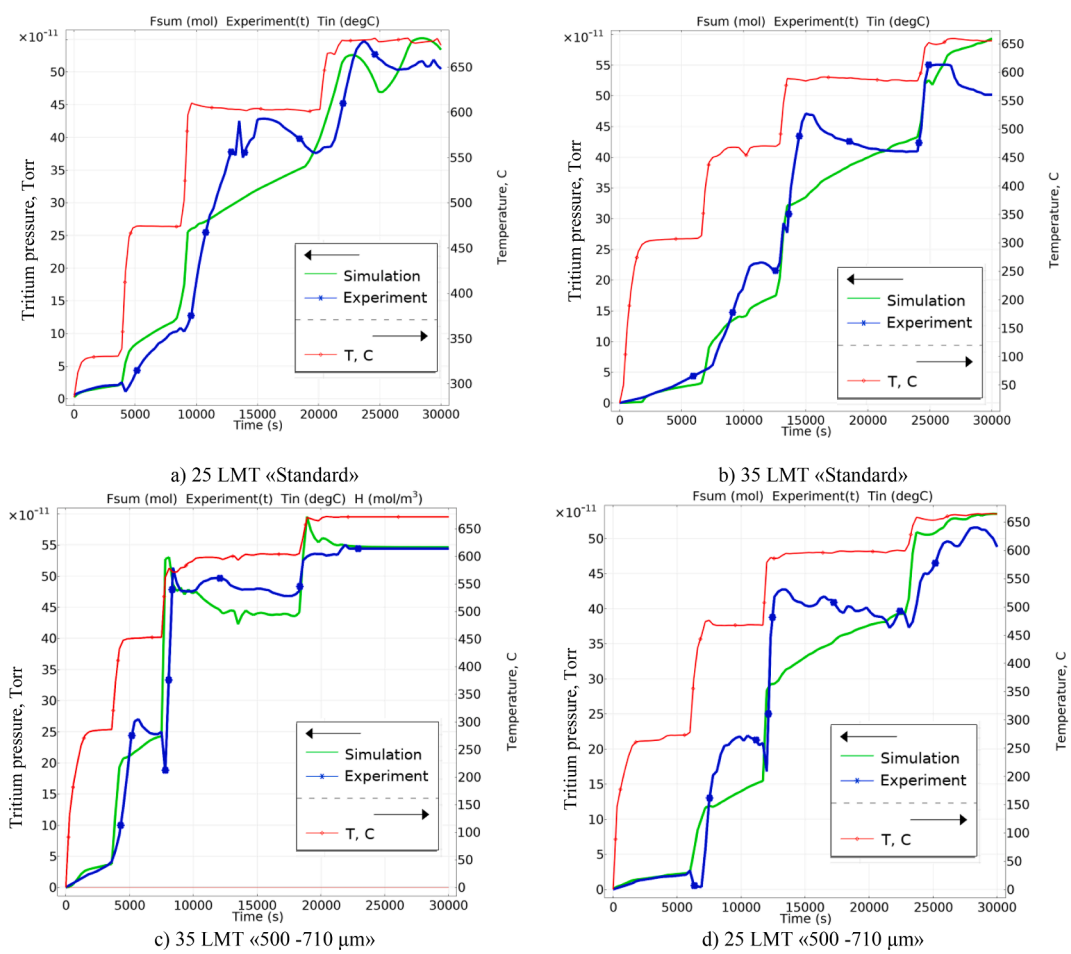

Fig. 10. Results of tritium (T_2) release simulation from biphasic lithium ceramics samples.

similar way: despite some differences in the diffusion and desorption parameters for ceramics of different types, the moment of equilibrium release of tritium from the irradiated samples occurs quite quickly, after which there is a uniform release of tritium throughout the entire irradiation time.

The data obtained indicating the effective release of tritium from the studied ceramics will not be a significant selection criterion for such ceramics; apparently, the parameters of the ceramics characterizing them from the point of view of mechanical resistance under conditions of prolonged exposure to high temperature and irradiation will be more significant here.

The results obtained in the experiments can be used in the analysis and selection of materials for solid ceramic breeder blankets.

CRediT authorship contribution statement

Timur Kulsartov: . **Zhanna Zaurbekova:** . **Regina Knitter:** . **Inesh Kenzhina:** Investigation, Validation. **Yevgen Chikhray:** . **Asset Shaimerdenov:** . **Saulet Askerbekov:** . **Gunta Kizane:** Resources, Supervision. **Alexandr Yelishenkov:** Investigation. **Timur Zholdybayev:** .

Declaration of competing interest

The authors declare that they have no known competing financial interests or personal relationships that could have appeared to influence the work reported in this paper.

Data availability

The authors are unable or have chosen not to specify which data has been used.

Acknowledgements

The research has been funded by the Science Committee of the Ministry of Science and Higher Education of the Republic of Kazakhstan with Program No. BR10965174.

References

[1] L.M. Giancarli, X. Bravo, S. Cho, M. Ferrari, T. Hayashi, B.Y. Kim, A. Leal-Pereira, J. P. Martins, M. Merola, R. Pascal, I. Schneiderova, Q. Sheng, A. Sircar, Y. Strebkov, J. van der Laan, A. Ying, Overview of recent ITER TBM Program activities, Fus. Eng. Des. 158 (2020) 111674, https://doi.org/10.1016/j.fusengdes.2020.111674.

[2] L.V. Boccaccini, G. Aiello, J. Aubert, C. Bachmann, T. Barrett, A. Del Nevo, D. Demange, L. Forest, F. Hernandez, P. Norajitra, G. Porempovic, D. Rapisarda, P. Sardain, M. Utili, L. Vala, Objectives and status of EUROfusion DEMO blanket studies, Fus. Eng. Des. 109–111 (Part B) (2016) 1199–1206, https://doi.org/10.1016/j.fusengdes.2015.12.054.

[3] F.A. Hernández, P. Pereslavtsev, G. Zhou, Q. Kang, S. D'Amico, H. Neuberger, L. V. Boccaccini, B. Kiss, G. Nádasi, L. Maqueda, I. Cristescu, I. Moscato, I. Ricapito, F. Cismondi, Consolidated design of the HCPB breeding blanket for the pre-conceptual design phase of the EU DEMO and harmonization with the ITER HCPB TBM program, Fus. Eng. Des. 157 (2020) 111614, https://doi.org/10.1016/j.fusengdes.2020.111614.

[4] O. Leys, J.M. Leys, R. Knitter, Current status and future perspectives of EU ceramic breeder development, Fus. Eng. Des. 164 (2021) 112171, https://doi.org/10.1016/j.fusengdes.2020.112171.

[5] Y. Wang, Q. Zhou, L. Xue, H. Li, Y. Yan, Synthesis of the biphasic mixture of Li2TiO3-Li4SiO4 and its irradiation performance, J. Eur. Ceram. Soc. 36 (2016) 4107–4113, https://doi.org/10.1016/j.jeurceramsoc.2016.04.005.

[6] M. Xiang, Y. Zhang, Y. Zhang, S. Liu, H. Liu, C. Wang, Fabrication and characterization of Li2TiO3eLi4SiO4 pebbles for tritium breeder, J. Fusion Energy 34 (2015) 1341–1347, https://doi.org/10.1007/s10894-015-9967-7.

[7] T. Hoshino, K. Kato, Y. Natori, F. Oikawa, N. Nakano, M. Nakamura, K. Sasaki, A. Suzuki, T. Terai, K. Tatenuma, Development of advanced tritium breeding material with added lithium for ITER-TBM, J. Nucl. Mater. 417 (2011) 684–687, https://doi.org/10.1016/j.jnucmat.2010.12.128.

[8] Y. Gan, F. Hernandez, D. Hanaor, R. Annabattula, M. Kamlah, P. Pereslavtsev, Thermal discrete element analysis of EU solid breeder blanket subjected to neutron irradiation, Fusion Sci. Technol. 66 (2014) 83–90, https://doi.org/10.13182/FST13-727.

[9] Y. Gan, M. Kamlah, H. Riesch-Oppermann, R. Rolli, P. Liu, Crush probability analysis of ceramic breeder pebble beds under mechanical stresses, J. Nucl. Mater. 417 (2011) 706–709, https://doi.org/10.1016/j.jnucmat.2010.12.131.

[10] S. Zhao, Y. Gan, M. Kamlah, T. Kennerknecht, R. Rolli, Influence of plate material on the contact strength of Li4SiO4 pebbles in crush tests and evaluation of the contact strength in pebble–pebble contact, Eng. Fract. Mech. 100 (2013) 28–37, https://doi.org/10.1016/j.engfracmech.2012.05.011.

[11] G. Ran, C. Xiao, X. Chen, Y. Gong, L. Zhao, H. Wang, X. Wang, Tritium release behavior of Li4SiO4 pebbles with high densities and large grain sizes, J. Nucl. Mater. 492 (2017) 189–194, https://doi.org/10.1016/j.jnucmat.2017.05.029.

[12] L. Zhao, X. Long, S. Peng, X. Chen, C. Xiao, G. Ran, J. Li, Tritium release in Li4SiO4 and Li4.2Si0.8Al0.2O4 ceramics, J. Nucl. Mater. 482 (2016) 42–46, https://doi.org/10.1016/j.jnucmat.2016.10.009.

[13] K. Munakata, A. Koga, Y. Yokoyama, S. Kanjo, S. Beloglazov, D. Ianovski, T. Takeishi, R.-D. Penzhorn, K. Kawamoto, H. Moriyama, Y. Morimoto, S. Akahori, K. Okuno, Effect of water vapor on tritium release from ceramic breeder material, Fusion Eng. Des. 69 (2003) 27–31, https://doi.org/10.1016/S0920-3796(03)00228-X.

[14] R. Knitter, M.H.H. Kolb, U. Kaufmann, A.A. Goraieb, Fabrication of modified lithium orthosilicate pebbles by addition of titania, J. Nucl. Mater. 442 (2013) S433–S436, https://doi.org/10.1016/j.jnucmat.2012.10.034.

[15] Q. Wang, Q. Zhou, Q. Xiong, J. Zhou, S. Li, S. Hirata, Y. Oya, Preparation of Li2TiO3-Li4SiO4-Pb tritium breeding ceramic and its mechanical properties, Ceram. Int. 48 (18) (2022) 26742–26749, https://doi.org/10.1016/j.ceramint.2022.05.369.

[16] M. Yang, L. Zhao, Y. Qin, G. Ran, Y. Gong, H. Wang, C. Xiao, X. Chen, T. Lu, Tritium release property of Li2TiO3-Li4SiO4 biphasic ceramics, J. Nucl. Mater. 538 (2020) 152268, https://doi.org/10.1016/j.jnucmat.2020.152268.

[17] M. Yang, L. Zhao, G. Ran, Y. Gong, H. Wang, S. Peng, C. Xiao, X. Chen, T. Lu, Tritium release behavior of Li2TiO3 and 2Li2TiO3-Li4SiO4 biphasic ceramic pebbles fabricated by microwave sintering, Fus. Eng. Des. 168 (2021) 112390, https://doi.org/10.1016/j.fusengdes.2021.112390.

[18] Q. Zhou, F. Sun, S. Hirata, S. Li, Y. Li, Y. Oya, Effect of neutron dose on the tritium release behavior of Li2TiO3–0.5Li4SiO4 biphasic ceramic, Int. J. Hydrog. Energy 48 (11) (2023) 4363–4370, https://doi.org/10.1016/j.ijhydene.2022.11.009.

[19] Q. Zhou, A. Togari, M. Nakata, M. Zhao, F. Sun, Q. Xu, Y. Oya, Release kinetics of tritium generation in neutron irradiated biphasic Li2TiO3–Li4SiO4 ceramic breeder, J. Nucl. Mater. 522 (2019) 286–293, https://doi.org/10.1016/j.jnucmat.2019.05.033.

[20] Qilai Zhou, Sicheng Li, Shiori Hirata, Asahi Sanfukuji, Guangfan Tan, Akira Taguchi, Yasuhisa Oya, Tritium and deuterium release behavior of Li2TiO3-0.5Li4SiO4–Pb ceramic, Ceram. Int. 49 (16) (2023) 26778–26785, https://doi.org/10.1016/j.ceramint.2023.05.214.

[21] Q. Qi, J. Wang, Q. Zhou, Y. Zhang, M. Zhao, S. Gu, G.-N. Luo, Comparison of tritium release behavior in Li2TiO3 and promising core-shell Li2TiO3–Li4SiO4 biphasic ceramic pebbles, J. Nucl. Mater. (2020) 152330, https://doi.org/10.1016/j.jnucmat.2020.152330.

[22] M.H.H. Kolb, R. Rolli, R. Knitter, Tritium adsorption/release behaviour of advanced EU breeder pebbles, J. Nucl. Mater. 489 (2017) 229–235, https://doi.org/10.1016/j.jnucmat.2017.03.051.

[23] T. Kulsartov, Z. Zaurbekova, R. Knitter, A. Shaimerdenov, Y. Chikhray, S. Askerbekov, A. Akhanov, I. Kenzhina, G. Kizane, Y. Kenzhin, M. Aitkulov, D. Sairanbayev, Studies of two-phase lithium ceramics Li4SiO4-Li2TiO3 under conditions of neutron irradiation, Nucl. Mater. Energ. 30 (2022) 101129, https://doi.org/10.1016/j.nme.2022.101129.

[24] T. Kulsartov, Zh Zaurbekova, R. Knitter, Ye. Chikhray, I. Kenzhina, S. Askerbekov, A. Shaimerdenov, G. Kizane, Reactor experiments on irradiation of two-phase lithium ceramics Li2TiO3/Li4SiO4 of various ratios, Fusion Eng. Des. 197 (2023), https://doi.org/10.1016/j.fusengdes.2023.114035.

[25] S. Pupeschi, M. Moscardini, Y. Gan, R. Knitter, M. Kamlah, Cyclic behavior of ceramic pebble beds under mechanical loading, Fusion Eng. Des. 134 (2018) 11–21.

[26] P. Blynskiy, et al., Experiments on tritium generation and yield from lithium ceramics during neutron irradiation, Int. J. of Hydrogen Energy 46 (13) (2021) 9186–9192.

[27] T. Kulsartov, et al., Determination of the activation energy of tritium diffusion in ceramic breeders by reactor power variation, Fusion. Eng. Des. 172 (2021) 112783.

[28] T. Kulsartov, et al., Modeling of hydrogen isotopes release from lithium ceramics Li2TiO3 during in-situ experiments using vacuum extraction method, Fusion. Eng. Des. 170 (2021) 112705.

[29] T. Kulsartov, et al., Features of the in-situ experiments on studying of tritium release from lithium ceramic Li2TiO3 using vacuum extraction method, Fusion. Eng. Des. 172 (2021) 112703.

[30] I. Kenzhina, T. Kulsartov, Y. Chikhray, Y. Kenzhin, Z. Zaurbekova, A. Shaimerdenov, G. Kizane, A. Zarins, A. Kozlovskiy, M. Gabdullin, A. Tolenova, Analysis of the reactor experiments results on the study of gas evolution from two-phase Li2TiO3-Li4SiO4 lithium ceramics, Nuclear Materials and Energy (2022) 101132. ToM 30.

[31] T. Kulsartov, Y. Kenzhin, R. Knitter, G. Kizane, Y. Chikhray, A. Shaimerdenov, S. Askerbekov, A. Akhanov, I. Kenzhina, Z. Zaurbekova, A. Zarins, D. Sairanbayev, Investigation of hydrogen and deuterium impact on the release of tritium from two-phase lithium ceramics under reactor irradiation, Nuclear Materials and Energy (2022) 101115. ToM 30.

[32] T. Kulsartov, A. Shaimerdenov, Z. Zaurbekova, R. Knitter, Y. Chikhray, S. Askerbekov, A. Akhanov, I. Kenzhina, M. Aitkulov, D.-K. Sairanbayev, Z. Bugubay, Investigation of transient processes of tritium release from biphasic

lithium ceramics Li4SiO4-Li2TiO3 at negative neutron flux pulse, Nuclear Materials and Energy 36 (2023) 101489, https://doi.org/10.1016/j.nme.2023.101489.

[33] Timur Kulsartov, Zhanna Zaurbekova, Yevgen Chikhray, Inesh Kenzhina, Saulet Askerbekov, Asset Shaimerdenov, Assyl Akhanov, Magzhan Aitkulov and Meiram Begentayev. Features of Helium and Tritium Release from Li2TiO3 Ceramic Pebbles under Neutron Irradiation // Materials. –2022. – 15(14). – 4741. https://doi.org/10.3390/ma15144741.

[34] COMSOL Multiphysics Simulation Software/Software Developers Website. Available online: https://www.comsol.com/comsol-multiphysics (accessed on 8 November 2023).